Electronic Supplementary Material (ESI) for Dalton Transactions.
This journal is © The Royal Society of Chemistry 2016

Designed Intramolecular Blocking of the SCO of an Fe(II) Complex

C. Bartual-Murgui,[a,]* S. Vela,[b,]* O. Roubeau[c] and G. Aromí[a,]*

Supporting Information

Synthesis

2-(3-phenyl-pyrazol-1-yl)-6-(1H-pyrazol-3-yl)pyridine (Ph1,3bpp). Ligand Ph1,3bpp was synthesized in three steps:

1-(6-(3-phenyl-pyrazol-1-yl)pyridin-2-yl)ethanone. To a solution of 1-(6-bromopyridin-2-yl)ethanone (1.6 g, 8 mmol) in toluene (10 mL) under N_2 were added 3-phenyl-1H-pyrazole (1.72 g, 12 mmol), 1,10-phenanthroline monohydrate (0.33 g, 1.65 mmol), CuI (0.16 g, 0.83 mmol) and K_2CO_3 (1.26 g, 8.29 mmol). The resulting black mixture was heated to reflux and vigorously stirred overnight (14 h). After cooling to room temperature, ethyl acetate (20 mL) and water (20 mL) were added and the organic layer isolated. The aqueous solution was extracted two additional times with ethyl acetate and the organic phases were recombined, washed with brine, dried with $MgSO_4$ and evaporated under vacuum to afford a brown powder of 1-(6-(3-phenyl-pyrazol-1-yl)pyridin-2-yl)ethanone. (yield; 1.74 g, 82%). ^{1}H NMR (400 MHz, $CDCl_3$, ppm): δ 2.71 (s, 3H), 6.77 (d, *J* = 2.7 Hz, 1H), 7.37 – 7.41 (m, 2H), 7.69 (d, *J* = 7.7 Hz, 1H), 7.83 – 8.95 (m, 4H), 8.22-8.26 (m, 1H), 8.60 (d, *J* = 2.6 Hz, 1H). Mass $(M + H)^+$ = 264.1.

1-(6-(3-phenyl-pyrazol-1-yl)-pyridin-2-yl)-3-(dimethylamino)prop-2-en-1-one. An excess of N,N-dimethylformamide-dimethyl acetal (1.7 g, 14 mmol) was added to 1-(6-(3-phenyl-pyrazol-1-yl)pyridin-2-yl)ethanone (1.8 g, 6.8 mmol) and the mixture was heated to reflux (110ºC) and stirred overnight. After cooling to room temperature, the resulting dark brown solution was concentrated under vacuum to obtain a brown solid of 1-(6-(3-phenyl-pyrazol-1-yl)-pyridin-2-yl)-3-(dimethylamino)prop-2-en-1-one (yield; 2.15 g, 99%). ^{1}H NMR (400 MHz, $CDCl_3$, ppm): δ 2.98 (s, 3H), 3.14 (s, 3H), 6.43 (d, *J* = 12.3 Hz, 1H), 6.74 (d, *J* = 2.6 Hz 1H), 7.39 (dd, *J* = 10.5, 4.9 Hz, 2H), 7.84 – 7.90 (m, 4H), 7.97 (dd, *J* = 14.3, 6.7 Hz, 2H), 8.12 (dd, *J* = 8.1, 0.9 Hz, 1H), 8.61 (d, *J* = 2.6 Hz, 1H). Mass $(M + H)^+$ = 319.1.

2-(1H-pyrazol-1-yl)-6-(1H-pyrazol-3-yl)pyridine (Ph1,3bpp). A large excess of hydrazine monohydrate (1.75 mL, 35 mmol) was added to an ethanolic solution (15 mL) of 1-(6-(3-phenyl-pyrazol-1-yl)pyridin-2-yl)-3-(dimethylamino)prop-2-en-1-one (2.15 g, 6.7 mmol) and the mixture stirred and refluxed overnight. The resulting solution was cooled to room temperature and evaporated under vacuum to afford a white powder identified as 2-(3-phenyl-pyrazol-1-yl)-6-(1H-pyrazol-3-yl)pyridine (yield; 1.2 g, 63 %). ^{1}H NMR (400 MHz, $CDCl_3$, ppm): δ 6.76 (d, J = 2.7 Hz, 1H), 6.81 (s, 1H), 7.26-7.33 (m, 1H), 7.36-7.41 (m, 2H), 653-7.64 (m, 2H), δ 7.92 – 7.78 (m, 3H), 7.99 (d, J = 8.1 Hz, 1H), 8.61 (d, J = 2.6 Hz, 1H). 10.55-11.02 (s, 1H). Mass $(M + H)^+$ = 288.0.

$[Fe(Ph1,3bpp)_2](ClO_4)_2·C_3H_6O$ (1a). A solution of Ph1,3bpp (0.025 g, 0.12 mmol) in dry acetone (10 mL) was added dropwise with stirring to a solution of $Fe(ClO_4)_2·6H_2O$ (0.023 g, 0.065 mmol) and ascorbic acid (~2 mg) in dry acetone (10 mL). The resulting yellow solution was stirred for 45−60 min at room temperature and, afterwards, filtered and layered with diethyl-ether (volume 1:1). Pale yellow plate crystals of **1a** were formed after 7 days of slow diffusion (yield, 40.7 %). EA, calcd (found) for $C_{37}H_{32}Cl_2FeN_{10}O_9$ (%): C 50.07 (48.60); H, 3.63 (3.38); N, 15.78 (15.50). Upon exposure to the atmosphere, crystals immediately begin a process of exchange of acetone by water, thus, the elemental analysis of the compound shows a lower than expected content of C.

$[Fe(Ph1,3bpp)_2](ClO_4)_2·½H_2O$ (1b). Exposure of **1a** to air for several weeks did not involve perceptible physical modifications on the lustrous yellow plate crystals. However, single crystal X-ray reveal the transformation of **1a** into **1b** following acetone by water exchange. EA, calcd (found) for $C_{68}H_{54}Cl_4Fe_2N_{20}O_{17}$ (%): C, 48.71 (48.41); H, 3.25 (3.10); N, 16.71 (16.52).

Computational Details.

All molecular geometries were optimized in the high-spin (HS) and low-spin states using the Quantum Espresso package (QE),[1] the PBE + U functional, with a Hubbard-like U parameter of 2.65 eV on the "d" orbitals of iron, the D2 correction of Grimme,[2] and Vanderbilt pseudopotentials. The molecules were introduced in a cubic cell of 60 Bohr^3 to isolate them from the virtual counterparts, which means all calculations simulate gas-phase conditions. This has been done with the help of the Makov-Payne approximation to treat the charged unit cells. The Hubbard term has been used to cure the incomplete cancellation of the electronic self-interaction in the PBE functional, which results in an unrealistic delocalization of orbitals.[3,4] The value U=2.65 eV has been found to be adequate to describe ΔH_{elec} in FeN_6-based compounds,[5] and used to explain the effect of solvent, ligand structure and solid-state packing in such architectures.[6,7] The evaluation of energy as a function of the dihedral angle in the Phenyl-Pyrrole system has been performed using the PBE functional, a 6-311+G(d) basis set, and the D2 correction of Grimme[2] as implemented in Gaussian 09.[8]

Physical Measurements.

Elemental analyses were performed at the Scientific and Technological Centers of the University of Barcelona using an elemental organic analyser Thermo EA Flash 200 working in recommended standard conditions.

Magnetic measurements were performed with a Quantum Design MPMS5 SQUID magnetometer at the "Unitat de mesures Magnètiques" of the Universitat de Barcelona. Diamagnetic corrections for the sample holder were applied as well as a correction for the diamagnetic contribution of the sample, as derived from Pascal's constants.

Thermogravimetric Analysis (TGA). Experiments were performed using a Mettler-Toledo TGA-851e thermos-balance. Samples were introduced in alumina crucibles of 70 mL volume and heated at 10 K/min from room temperature to 230ºC under a dry nitrogen atmosphere.

Nuclear Magnetic Resonance Spectroscopy. H^1NMR spectra were registered at room temperature with a Varian Inova 300 MHz instrument at the “Unitat de RMN” of the Universitat de Barcelona.

Mass Spectroscopy spectra were recorded using an Agilent 1100 LC/MSD-TOF instrument operating in the positive electrospray Ionization mode (4KV, fragmentor = 175.0 V, gas temperature = 325ºC, nebulizing gas: N_2 Pressure = 15 psi, drying gas: N_2 Flow = 7.0 l/min). The samples were introduced into the source with a HPLC system using a mixture of H_2O:CH_3CN (1:1) as eluent (200 μl/min).

Single Crystal X-ray Diffraction (SCXRD).

Data were collected at 100 K on a Bruker APEXII QUAZAR diffractometer equipped with a microfocus multilayer monochromator with MoKα radiation (λ = 0.71073 Å) on a yellow plate with dimensions 0.30 x 0.12 x 0.04 mm^3 and a yellow plate with dimensions 0.31 x 0.14 x 0.03 mm^3, respectively for **1a** and **1b**. Data reduction and absorption corrections were performed with SAINT and SADABS, respectively.[9] The structures were solved by intrinsic phasing with SHELXT[10] and refined by full-matrix least-squares on F^2 with SHELXL-2014.[11] Both structures were refined as two-component inversion twins. All details can be found in CCDC 1492563-1492564 (**1a**-**1b**) that contain the supplementary crystallographic data for this paper. These data can be obtained free of charge from The Cambridge Crystallographic Data Center via https://summary.ccdc.cam.ac.uk/structure-summary-form. Crystallographic and refinement parameters are summarized in Table S1. Selected bond lengths and angles and intermolecular distances are given in Tables S2 and S3.

Table S1. Crystallographic and refinement parameters for the structures of compounds **1a** and **1b**.

Compound	**1a**	**1b**
Formula	$C_{37}H_{32}Cl_2FeN_{10}O_9$	$C_{68}H_{54}Cl_4Fe_2N_{20}O_{17}$
FW (g mol^{-1})	887.47	1676.81
Wavelength (Å)	0.71073	
T (K)	100	
Crystal system	orthorhombic	orthorhombic
Space group	$Pca2_1$	$Pna2_1$
a (Å)	20.9317(10)	20.841(3)
b (Å)	8.5496(5)	8.5350(10)
c (Å)	43.116(2)	39.946(6)
α (°)	90	90
β (°)	90	90
γ (°)	90	90
V (Å^3)	7715.9(7)	7105.5(17)
Z	8	4
ρ_{calcd} (g cm^{-3})	1.528	1.567
μ (mm^{-1})	0.599	0.645
Independent reflections (R_{int})	17904 (0.1130)	11405 (0.0739)
Restraints / Parameters	149 / 1068	307 / 1036
Goodness-of-fit on F^2	1.051	1.112
Final R_1 / wR_2 [I>2σ(I)]	0.0769 / 0.1939	0.0780 / 0.1749
Final R_1 / wR_2 [all data]	0.1005 / 0.2125	0.1033 / 0.1870
Largest diff. peak and hole (e Å^3)	1.273 / –2.746	0.615 / –1.110

Table S2. Selected bond lengths (Å) and angles (º) describing the coordination environments of the Fe sites in the structures of compounds **1a** and **1b**.

	1a	**1b**
Fe1–N3	2.117(6)	2.114(11)
Fe1–N8	2.135(8)	2.138(11)
Fe1–N10	2.166(6)	2.154(11)
Fe1–N6	2.180(6)	2.176(12)
Fe1–N1	2.185(6)	2.189(11)
Fe1–N5	2.201(6)	2.221(11)
Fe2–N18	2.125(6)	2.144(12)
Fe2–N13	2.135(7)	2.120(11)
Fe2–N15	2.165(6)	2.214(12)
Fe2–N11	2.189(6)	2.179(12)
Fe2–N16	2.189(6)	2.188(13)
Fe2–N20	2.207(6)	2.153(12)
N3–Fe1–N10	115.4(3)	116.1(5)
N8–Fe1–N10	73.3(3)	73.3(5)
N3–Fe1–N6	97.4(2)	97.0(4)
N8–Fe1–N6	73.8(3)	73.5(4)
N3–Fe1–N1	74.5(2)	74.2(4)
N8–Fe1–N1	100.4(2)	100.6(4)
N10–Fe1–N1	99.6(2)	99.2(4)
N6–Fe1–N1	86.2(2)	86.8(4)
N3–Fe1–N5	73.4(2)	73.2(4)
N8–Fe1–N5	112.7(2)	113.2(4)
N10–Fe1–N5	85.4(2)	86.0(4)
N6–Fe1–N5	107.5(2)	107.2(4)
N3–Fe1–N8	170.3(2)	169.6(4)
N10–Fe1–N6	147.1(2)	146.8(4)
N1–Fe1–N5	146.4(2)	145.8(4)
N18–Fe2–N15	116.7(2)	112.1(4)
N13–Fe2–N15	72.5(3)	73.8(4)
N18–Fe2–N11	97.2(2)	101.0(4)
N13–Fe2–N11	73.4(3)	73.9(4)
N18–Fe2–N16	73.9(2)	73.1(5)
N13–Fe2–N16	101.1(2)	97.4(4)
N15–Fe2–N16	100.2(2)	107.9(4)
N11–Fe2–N16	85.3(2)	83.9(5)
N18–Fe2–N20	73.5(2)	73.5(5)
N13–Fe2–N20	112.6(2)	116.0(5)
N15–Fe2–N20	86.0(2)	85.3(4)
N11–Fe2–N20	108.1(2)	101.9(5)
N18–Fe2–N13	169.9(3)	169.8(5)
N15–Fe2–N11	145.9(2)	146.8(4)
N16–Fe2–N20	146.0(2)	146.5(5)

Table S3. Distances and angles describing the hydrogen bonds in the structures of compounds **1a** and **1b**.

D–H···A	D–H (Å)	H···A (Å)	D···A (Å)	D–H···A (º)
1a				
N2 H2B O1S	0.88	1.93	2.792(8)	164.4
N7 H7B O1#1	0.88	1.96	2.800(9)	159.8
N12 H12A O13#2	0.88	1.94	2.796(9)	164.2
N17 H17B O2S#3	0.88	1.91	2.769(9)	164.3
1b				
N2 H2B O1W	0.88	1.97	2.828(16)	164.7
N7 H7B O2	0.88	1.96	2.805(16)	161.8
N12 H12A O9	0.88	1.98	2.826(17)	162.0
N17 H17B O13	0.88	1.96	2.806(16)	161.7
O1W H1W O11	0.90(3)	2.03(4)	2.932(17)	173(17)
O1W H2W O8B	0.91(3)	2.07(5)	2.87(3)	146(10)
O1W H2W O8	0.91(3)	2.29(12)	2.96(2)	130(12)

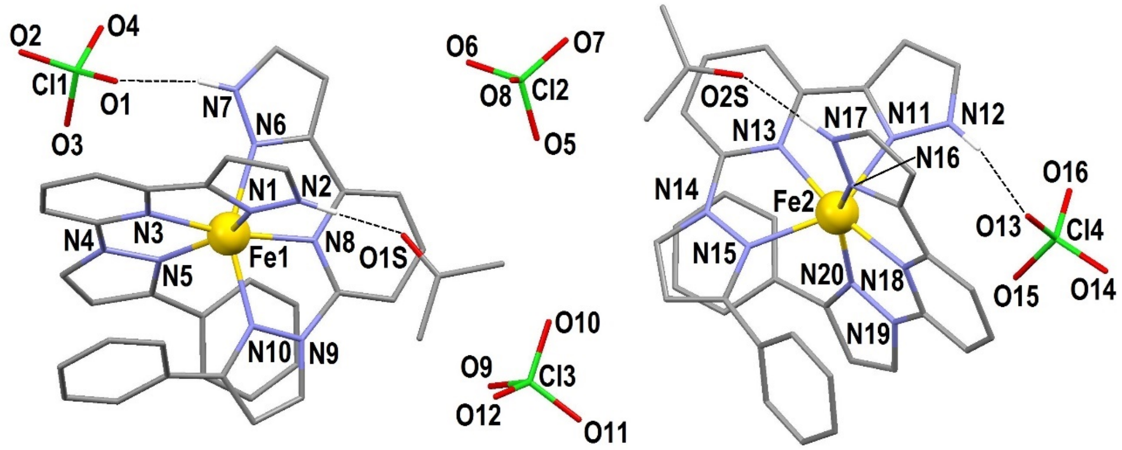

Figure S1. Labelled representation of the asymmetric unit of [Fe(Ph1,3bpp)$_2$](ClO$_4$)$_2$·C$_3$H$_6$O (**1a**), emphasizing the intramolecular H-bond interactions as black dashed lines. Only H atoms involved in H-bonds shown. C and H atoms are not labelled.

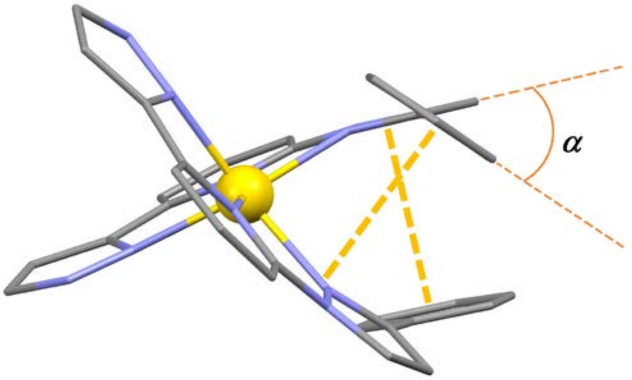

Figure S2. Representation of [Fe(Ph1,3bpp)$_2$]$^{2+}$ in **1a** and **1b**, emphasizing the torsion angle, *α*, between the phenyl substituent and the carrier pyrazol-1-yl ring as well as the π···π interactions between the phenyl substituent and the opposite 1,3bpp moiety.

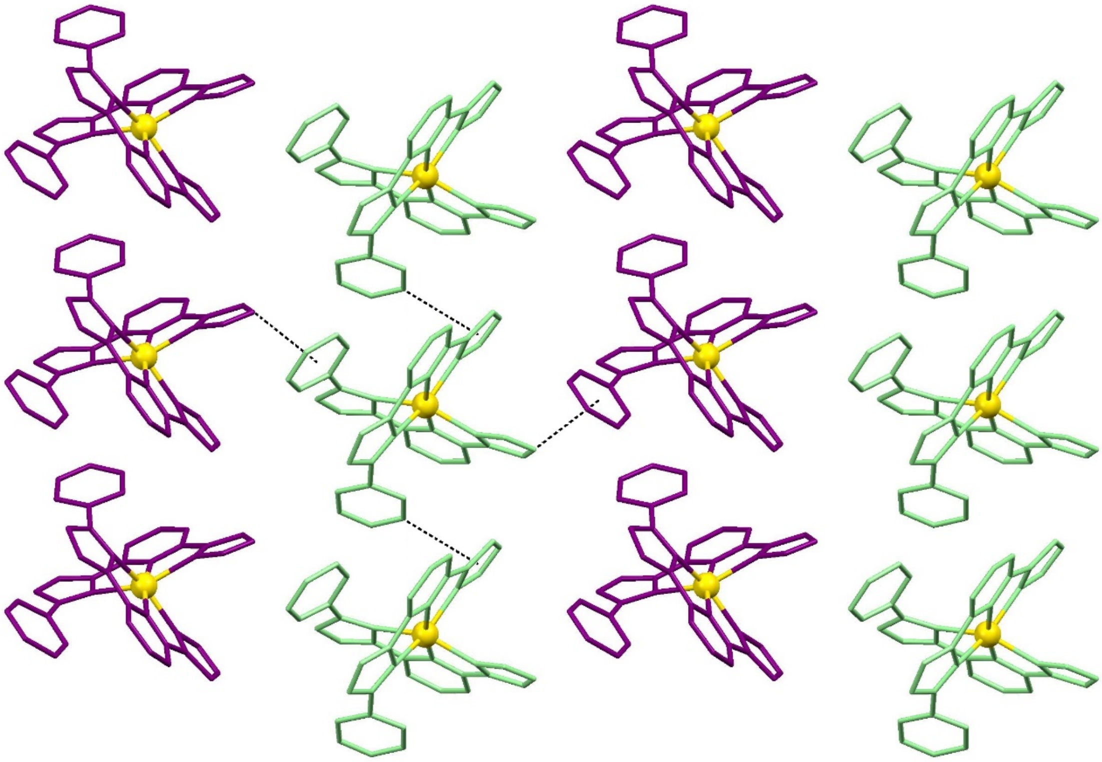

Figure S3. Sheets of $[Fe(Ph1,3bpp)_2]^{2+}$ complexes within **1a** and **1b**, with both enantiomers shown in different colors, showing C–H···π interactions between them.

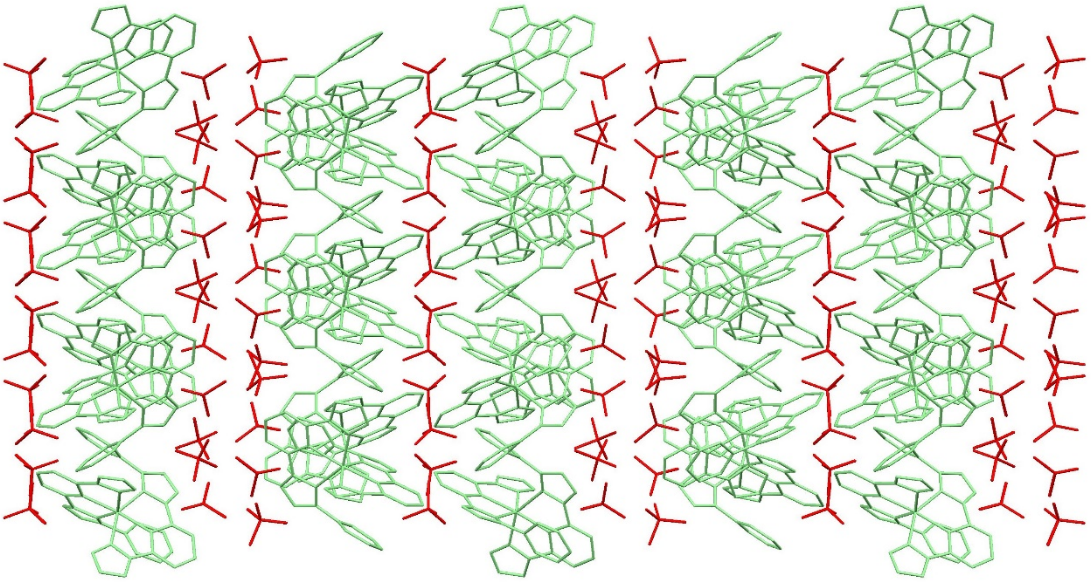

Figure S4. View of **1a**, down the crystallographic *a* axis, showing alternating layers of $[Fe(Ph1,3bpp)_2]^{2+}$ complexes (green) and acetone/ClO_4^- species (red).

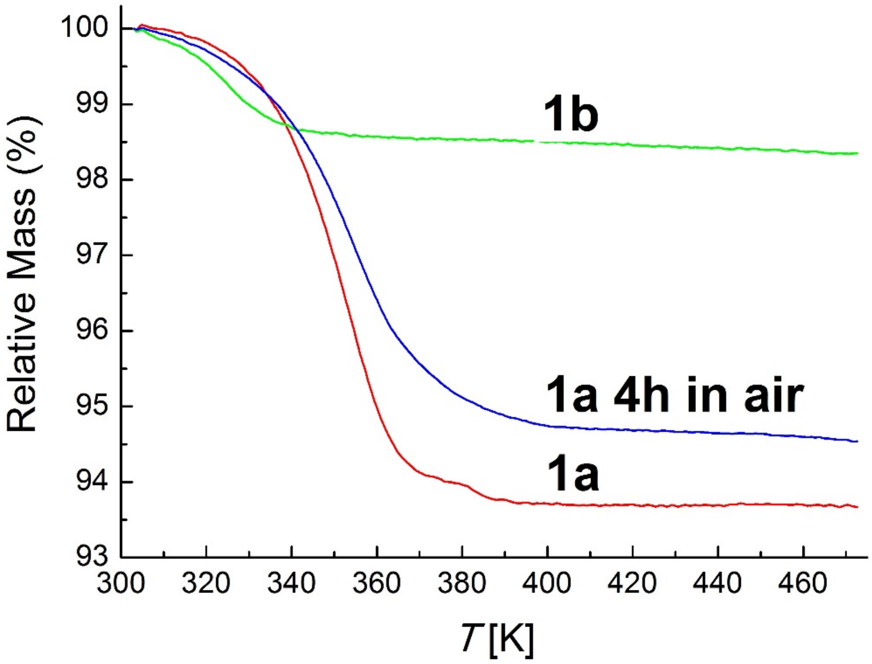

Figure S5. TGA analysis of **1a**, showing the loss of one molecule of acetone (6.3% at 400 K; calcd. 6.5%) per Fe(II) complex, **1a** after 4h of exposure to the atmosphere, indicating that the acetone/water exchange has begun (5.5% loss at 400 K), and **1b** (as obtained by exposing **1a** to the atmosphere for 40 days), showing loss of half molecule of water per Fe(II) complex (1.4% at 350 K; calcd. 1.1%), which confirms that complete substitution of acetone by one half the molar amount of water has taken place.

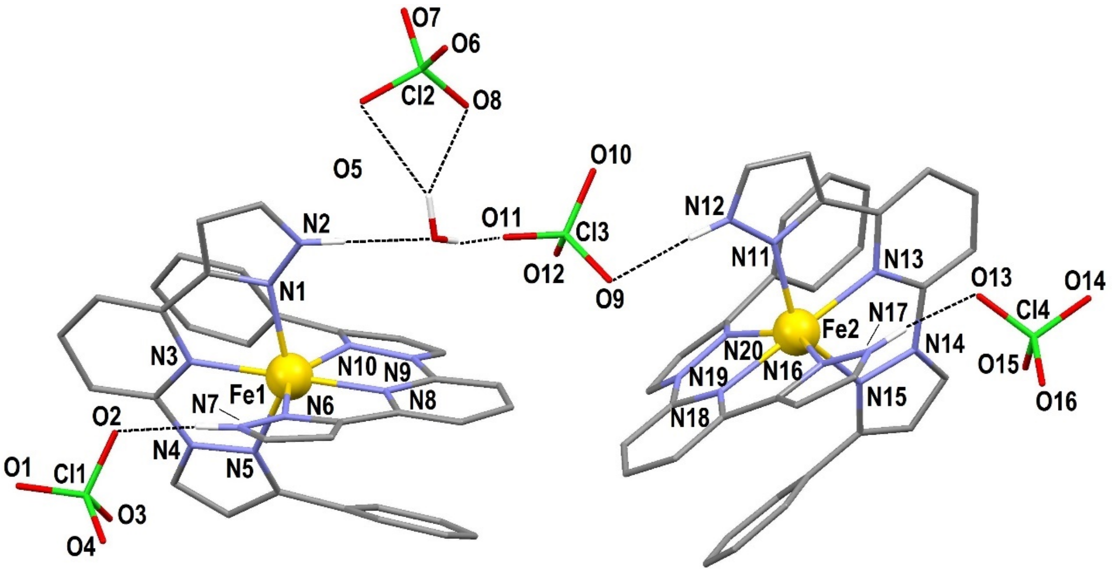

Figure S6. Labelled representation of the asymmetric unit of [Fe(Ph1,3bpp)$_2$](ClO$_4$)$_2$·0.5H$_2$O (**1b**), emphasizing the intramolecular H-bond interactions as black dashed lines. Only H atoms involved in H-bonds shown. C and H atoms are not labelled

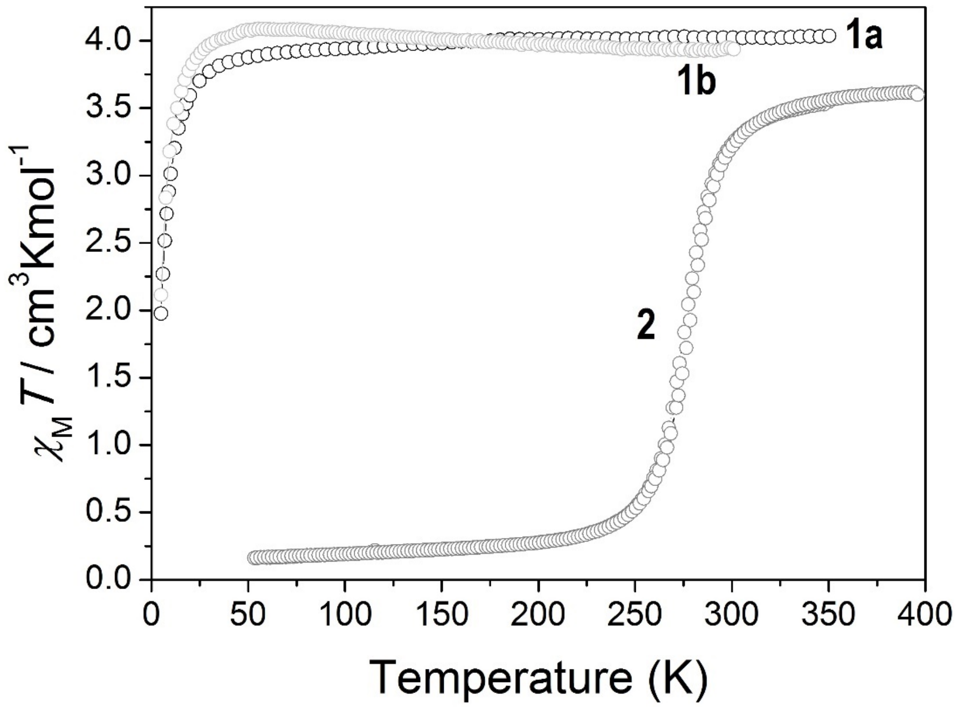

Figure S7. $\chi_M T$ *vs. T* plot for compounds [Fe(Ph1,3bpp)$_2$] (ClO$_4$)$_2$·C$_3$H$_6$O (**1a**) and [Fe(Ph1,3bpp)$_2$] (ClO$_4$)$_2$·0.5H$_2$O (**1b**) as well as for the related complex [Fe(1,3bpp)$_2$](ClO$_4$)$_2$ (**2**) for comparison, the latter taken from reference 28.

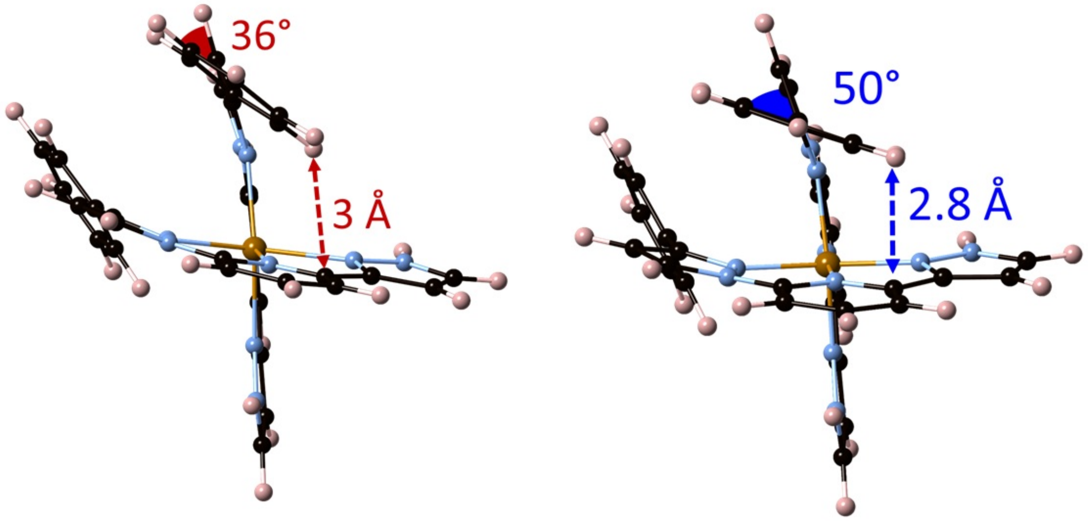

Figure S8. Representation of the optimized structures **1**$_{HS}$ and **1**$_{LS}$. The phenyl-pyrazole-3-yl torsion angle and the closest inter-ligand contact have been highlighted.

References

(1) Giannozzi, P.; Baroni, S.; Bonini, N.; Calandra, M.; Car, R.; Cavazzoni, C.; Ceresoli, D.; Chiarotti, G. L.; Cococcioni, M.; Dabo, I.; Corso, A. D.; Gironcoli, S. d.; Fabris, S.; Fratesi, G.; Gebauer, R.; Gerstmann, U.; Gougoussis, C.; Kokalj,

A.; Lazzeri, M.; Martin-Samos, L.; Marzari, N.; Mauri, F.; Mazzarello, R.; Paolini, S.; Pasquarello, A.; Paulatto, L.; Sbraccia, C.; Scandolo, S.; Sclauzero, G.; Seitsonen, A. P.; Smogunov, A.; Umari, P.; Wentzcovitch, R. M. *J. Phys.: Condens. Matter* **2009**, *21*, 395502.

(2) Grimme, S. *J. Comput. Chem.* **2006**, *27*, 1787.

(3) Scherlis, D. A.; Cococcioni, M.; Sit, P.; Marzari, N. *J. Phys. Chem. B* **2007**, *111*, 7384.

(4) Liechtenstein, A. I.; Anisimov, V. I.; Zaanen, J. *Phys. Rev. B* **1995**, *52*, R5467.

(5) Vela, S.; Fumanal, M.; Ribas-Arino, J.; Robert, V. *Phys. Chem. Chem. Phys.* **2015**, *17*, 16306.

(6) Vela, S.; Gourlaouen, C.; Fumanal, M.; Ribas-Arino, J. *Magnetochemistry* **2016**, *2*, 6.

(7) Vela, S.; Novoa, J. J.; Ribas-Arino, J. *Phys. Chem. Chem. Phys.* **2014**, *16*, 27012.

(8) Frisch, M. J.; Trucks, G. W.; Schlegel, H. B.; Scuseria, G. E.; Robb, M. A.; Cheeseman, J. R.; Scalmani, G.; Barone, V.; Mennucci, B.; Petersson, G. A.; Nakatsuji, H.; Caricato, M.; Li, X.; Hratchian, H. P.; Izmaylov, A. F.; Bloino, J.; Zheng, G.; Sonnenberg, J. L.; Hada, M.; Ehara, M.; Toyota, K.; Fukuda, R.; Hasegawa, J.; Ishida, M.; Nakajima, T.; Honda, Y.; Kitao, O.; Nakai, H.; Vreven, T.; Montgomery Jr., J. A.; Peralta, J. E.; Ogliaro, F.; Bearpark, M.; Heyd, J. J.; Brothers, E.; Kudin, K. N.; Staroverov, V. N.; Kobayashi, R.; Normand, J.; Raghavachari, K.; Rendell, A.; Burant, J. C.; Iyengar, S. S.; Tomasi, J.; Cossi, M.; Rega, N.; Millam, J. M.; Klene, M.; Knox, J. E.; Cross, J. B.; Bakken, V.; Adamo, C.; Jaramillo, J.; Gomperts, R.; Stratmann, R. E.; Yazyev, O.; Austin, A. J.; Cammi, R.; Pomelli, C.; Ochterski, J. W.; Martin, R. L.; Morokuma, K.; Zakrzewski, V. G.; Voth, G. A.; Salvador, P.; Dannenberg, J. J.; Dapprich, S.; Daniels, A. D.; Farkas, Ö.; Foresman, J. B.; Ortiz, J. V.; Cioslowski, J.; Fox, D. J.; CT., G. I. W., Ed. 2009.

(9) .G. M. Sheldrick, 2012, *SAINT and SADABS*, Bruker AXS Inc., Madison, Wisconsin, USA.

(10) G. M. Sheldrick, *Acta Cryst. A*, 2015, **71**, 3-8.

(11) G. M. Sheldrick, *Acta Cryst. C*, 2015, **71**, 3-8.